$$e_o = \sum_{i=0}^{n} a_i e_{in}(t-iT) \qquad (C-25)$$

$$i=0,1,\ldots n$$

where:

a_i = Binomial weighting factors, $(-1)^i \binom{n}{i}$

Therefore, the impulse response of a first-order nonrecursive filter to a single pulse is given by:

$$e_o = e_{in}(t) - e_{in}(t-T) \qquad (C-26)$$

Noise

The rms noise transfer properties of a single stage MTI canceller is:

$$n_{MTI_{lo}} = \sqrt{a_o{}^2 n_{MTI_{li}}{}^2 + a_i{}^2 n_{MTI_{li}}{}^2} \qquad (C-27a)$$

$$= \sqrt{2}\, n_{MTI_{li}} \qquad (C-27b)$$

Thus, the noise power transfer function of a single stage MTI canceller is:

$$N_{MTI_{lo}} = N_{MTI_{li}} + 3 \text{ dB} \qquad (C-28)$$

Desired Signal

For a desired signal (synchronous signal), the signal power transfer gain for a single stage MTI canceller when averaged over all possible doppler frequencies is 3 dB (Nathanson, 1969). Since the noise power density is uniform over the MTI filter, the filter treats both noise and signal (on the average) alike. Thus, there is also a 3 dB power transfer gain in both noise and desired signal in a first-order MTI filter. Hence, the signal-to-noise ratio (SNR) at the MTI canceller output is the same as at the input to the MTI canceller.

Interfering Signal

For an asynchronous interfering signal, the number of interfering pulses is increased by a factor of two for a single stage MTI canceller, resulting in an increase in the interfering signal average power. The asynchronous interfering signal bipolar output is converted back to unipolar resulting in two positive output pulses for each asynchronous input pulse. Figure C-11 shows an aysnchronous interfering signal output measured on an ASR-8 operating in the CANC 1 mode. Equation C-26 indicates that the interfering signal peak power transfer properties of a single stage MTI canceller is given by:

$$I_{MTI_{1o}} = I_{MTI_{1i}} \qquad \text{(C-29)}$$

Using Equations C-28 and C-29, the INR transfer properties of a single stage MTI canceller for asynchronous interference are given by:

$$INR_{MTI_{1o}} = INR_{MTI_{1i}} - 3 \text{ dB} \qquad \text{(C-30)}$$

Double Stage Canceller Transfer Properties

Figure C-12 shows a block diagram of a double stage MTI canceller with feedback (second-order recursive filter). The canonical form of the double stage canceller with feedback is shown in Figure C-13. Different modes of MTI canceller operation are obtained by varying the feedback coefficients (b_1 and b_2). By changing the feedback coefficients, the doppler frequency response of the MTI filter is shaped to permit improvement in the subclutter visibility (SCV). TABLE C-1 shows the canonical feed-forward coefficients (a_o, a_1, a_2) and feedback coefficients (b_1 and b_2) for the different modes of operation of the double stage cancellers in the ASR-7 and ASR-8. The Z-Transfer function of the second-order recursive filter is given by:

$$H(Z) = \frac{e_o}{e_{in}} = \frac{a_o + a_1 Z^{-1} + a_2 Z^{-2}}{b_1 Z^{-1} + b_2 Z^{-2}} \qquad \text{(C-31)}$$

where:

Z^{-1} = Unit delay, (t- T)

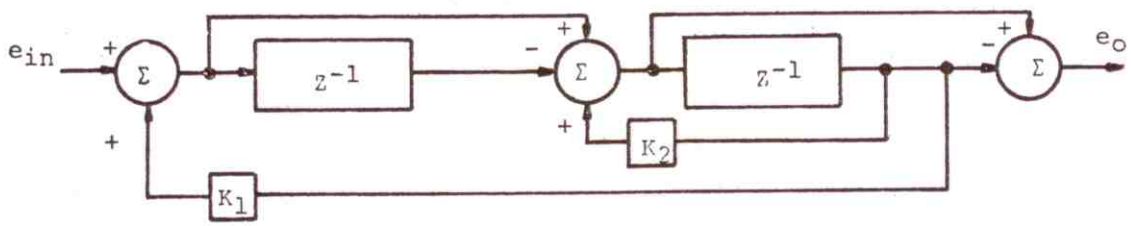

Figure C-12. Second-Order MTI Filter with Feedback for Velocity Shaping

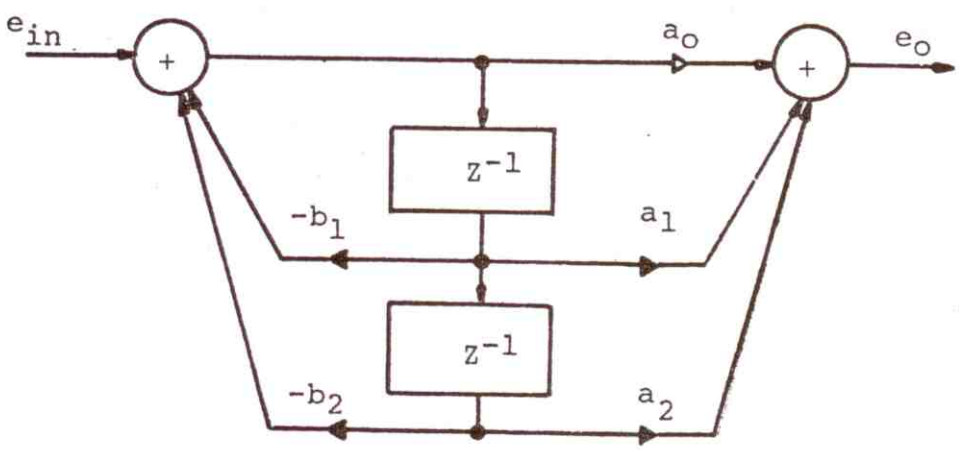

Figure C-13. Canonical Form of Second-Order Recursive Filter

TABLE C-1

MTI CANCELLER TRANSFER PROPERTIES

MTI MODE	FEED-FORWARD COEFFICIENTS			FEEDBACK COEFFICIENTS		NOISE GAIN		PEAK INTERFERENCE GAIN		PEAK INR (dB)
	a_o	a_1	a_2	b_1	b_2	VOLTS	dB	VOLTS	dB	
CANC 1	1	-1	0	0	0	$\sqrt{2}$	3	1.0	0	-3
1&2 CASC	1/2	-1	1/2	0	0	$\sqrt{1.5}$	1.76	1.0	0	-1.76
SCV-25	1/2	-1	1/2	1 1/4	-1/2	$\sqrt{0.454}$	-3.42	0.50	-6.0	-2.58
SCV-30	1/2	-1	1/2	1	-1/2	$\sqrt{0.6}$	-2.21	0.50	-6.0	-3.79
SCV-35	1/2	-1	1/2	3/4	-1/2	$\sqrt{0.777}$	-1.09	0.625	-4.08	-2.99
SCV-40	1/2	-1	1/2	1/2	-1/2	1.0	0	0.75	-2.49	-2.49

T = Radar pulse period, in seconds

a_i = Binomial weighting factors, $(-1)^i \binom{n}{i}$

n = filter order, 2

b_i = Canonic feedback factors

The binomial weighting factors are 1, -2, and 1 for a second order filter. However, on some of the new digital radars binomial weighting factors (feed-forward coefficients) of 1/2, -1, and 1/2 are used to reduce word size. Equation C-21 can be rewritten using the non-canonic feedback coefficient (K_1 and K_2):

$$H(Z) = \frac{e_o}{e_{in}} = \frac{a_o + a_1 Z^{-1} + a_2 Z^{-2}}{1-(K_1 + K_2)Z^{-1} + K_1 Z^{-2}} \qquad \text{(C-32)}$$

The frequency response magnitude of the second-order recursive filter transfer function is determined by letting $Z^{-1} = e^{-j\omega_d T}$ and is given by:

$$|H(e^{j\omega T})| = \frac{\sin^4 \frac{(\omega_d T)}{2}}{[1+(K_1+K_2)+K_1^2]-2(1+K_1)(K_1+K_2)\cos \omega_d T+2K_1 \cos 2\omega_d T} \qquad \text{(C-33)}$$

where:

ω_d = Doppler frequency of return signal, in radians per second

K_1 and K_2 = Feedback constants

Figure C-14 shows the frequency response characteristics and improvement factor for several feedback constants for a second-order recursive filter.

For the non-feedback MTI canceller mode (1 and 2 CASC, b_1 and $b_2 = 0$) the MTI filter has no poles, and Equation C-31 reduces to:

$$H(Z) = \frac{e_o}{e_{in}} = a_o + a_1 Z^{-1} + a_2 Z^{-2} \qquad \text{(C-34)}$$

Therefore, the MTI canceller output response becomes:

$$e_o = a_o e_{in}(t) + a_1 e_{in}(t-T) + a_2 e_{in}(t-2T) \qquad \text{(C-35)}$$

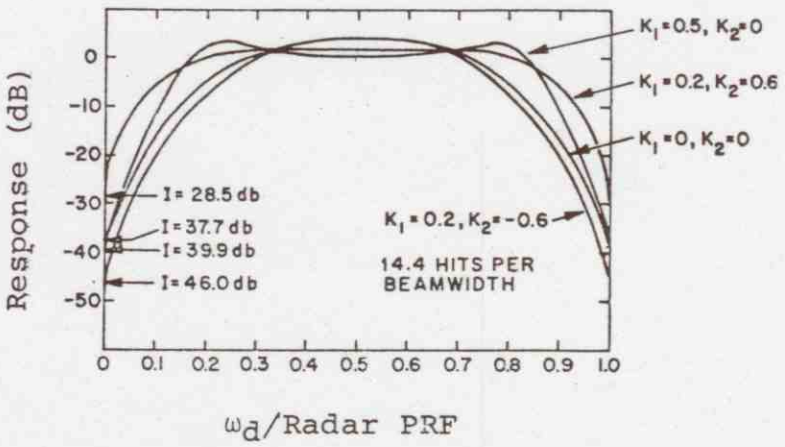

Figure C-14. Frequency Response for a Double Stage Canceller with Feedback

Noise

The rms noise transfer properties of a double stage MTI canceller for the non-feedback mode (b_1 and $b_2 = 0$) is given by:

$$n_{MTI_{2o}} = \sqrt{a_o^2 n_{MTI_{2i}}^2 + a_1^2 n_{MTI_{2i}}^2 + a_2^2 n_{MTI_{2i}}} \qquad \text{(C-36a)}$$

$$= \sqrt{1.5}\, n_{MTI_{2i}}; \quad \text{for } a_i = \tfrac{1}{2}, -1, \text{ and } \tfrac{1}{2} \qquad \text{(C-36b)}$$

$$= \sqrt{6}\, n_{MTI_{2i}}; \quad \text{for } a_i = 1, -2, \text{ and } 1 \qquad \text{(C-36c)}$$

Thus, the noise power transfer function of a double stage MTI canceller is:

$$N_{MTI_{2o}} = N_{MTI_{2i}} + 1.8 \text{ dB; for } a_i = \tfrac{1}{2}, -1, \text{ and } \tfrac{1}{2} \qquad \text{(C-37a)}$$

$$N_{MTI_{2o}} = N_{MTI_{2i}} + 7.8 \text{ dB; for } a_i = 1, -2, \text{ and } 1 \qquad \text{(C-37b)}$$

For the MTI canceller feedback modes of operation the rms noise transfer properties are determined using a recursive algoritnm. The noise power transfer properties for the different feedback modes were obtained by simulation (see Appendix E), and are shown in TABLE C-1.

The noise amplitude distribution at the canceller output is Gaussian distributed with a zero mean. Since the MTI canceller sums the noise at the input to the canceller which has a Gaussian amplitude distribution, the output noise amplitude distribution is also Gaussian.

Desired Signal

For desired signal (synchronous signal), the signal power transfer gain for a double stage MTI canceller without feedback or with feedback when averaged over all possible doppler frequencies is the same as the noise power transfer gain (see noise gain in TABLE C-1). Since the noise power density is uniform over the MTI filter, the filter treats both noise and signal (on the average) alike. Thus the signal-to-noise ratio (SNR) at the MTI canceller output is the same as at the input to the canceller when averaged over all possible doppler frequencies.

Interfering Signal

For an asynchronous interfering signal, a double stage MTI canceller will produce several interfering signal pulses at the canceller output for each interfering pulse at the MTI canceller input. These interfering pulses at the MTI canceller output are synchronous with the radar system (i.e., fall in the same range bin in successive azimuth change pulses). The amplitude of these pulses produced by a single interfering pulse are a function of the feed-forward coefficients (a_o, a_1, a_2) and the feedback coefficients (b_1 and b_2).

For the non-feedback MTI canceller mode (1 and 2 CASC, b_1 and b_2 = 0), the response of a double stage MTI canceller to a single interfering pulse is given in Equation C-35. Therefore, each interfering pulse produces three synchronous interfering pulses. Equation C-35 indicates that the interfering signal peak power transfer properties of a double stage MTI canceller due to the binomial weighting factors (feed-forward coefficients) is given by:

$$I_{MTI_{2o}} = I_{MTI_{2i}} \quad ; \text{ for } a_i = \tfrac{1}{2}, -1, \text{ and } \tfrac{1}{2} \qquad \text{(C-38a)}$$

$$I_{MTI_{2o}} = I_{MTI_{2i}} + 6 \text{ dB}; \text{ for } a_i = 1, -2, \text{ and } 1 \qquad \text{(C-38b)}$$

Figure C-15 shows a photograph of a MTI canceller output measured on an ASR-8 operating in the 1 and 2 CASC mode. The center pulse in Figure C-15 is twice the amplitude of the first and third pulses due to the binomial weighting factors of 1/2, -1, and 1/2. Figure C-16 shows a simulated MTI canceller output for the 1 and 2 CASC mode, and a four volt interfering pulse. The two additional pulses generated by the MTI canceller are synchronous with the radar PRF.

Using Equations C-37 and C-38, the INR transfer properties of a double stage MTI canceller in non-feedback mode for a_i = 1/2, -1, and 1/2 or 1, -2, and 1 are given by:

$$INR_{MTI_{2o}} = INR_{MTI_{2i}} - 1.8 \text{ dB} \qquad \text{(C-39)}$$

The double stage MTI canceller output response after rectification to an interfering pulse for various feedback modes of operation were simulated and are shown in Figures C-17 through C-20. The simulated responses are for a four volt interfering signal at the MTI canceller input. The figures show that when operating in the feedback mode, there are more than three pulses out for each interfering pulse. However, by the third or fourth pulse, the interfering signal is down below noise level (1 volt) depending on the feedback constants and interfering signal level. The interfering signal peak

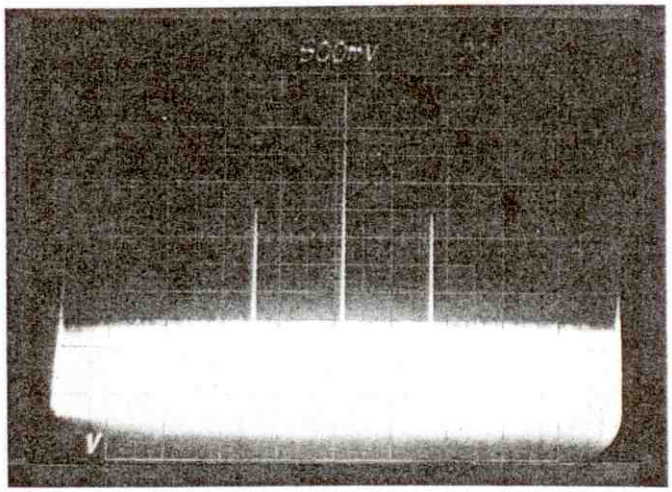

Figure C-15. Measured Double Stage MTI Canceller Response to an Interfering Pulse (1&2 CASC Mode)

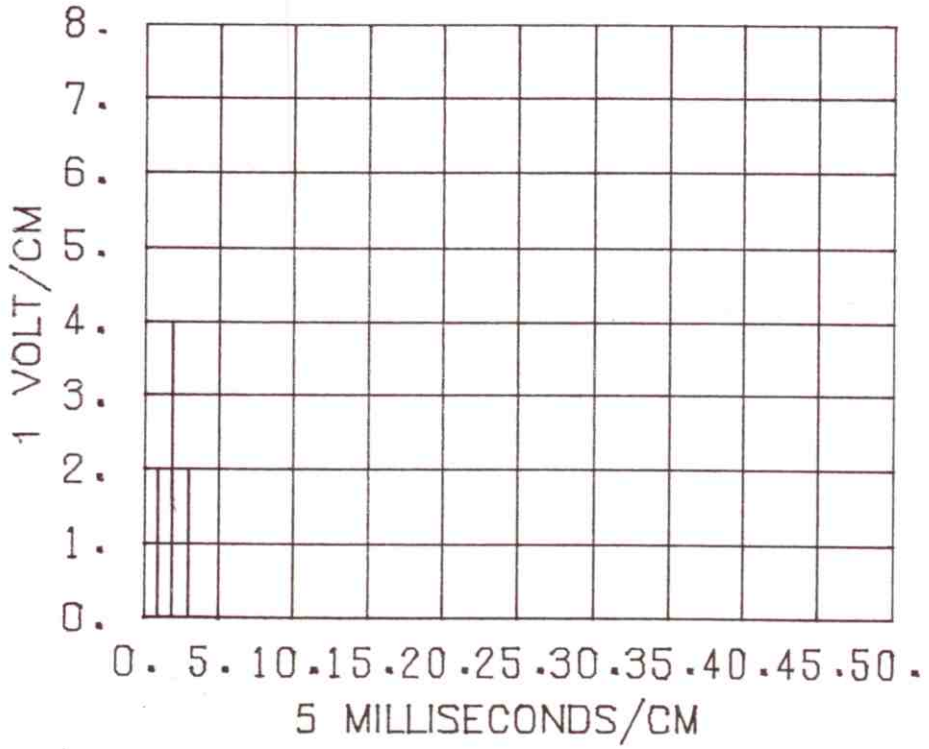

Figure C-16. Simulated Double Stage MTI Canceller Response to an Interfering Pulse (1&2 CASC Mode)

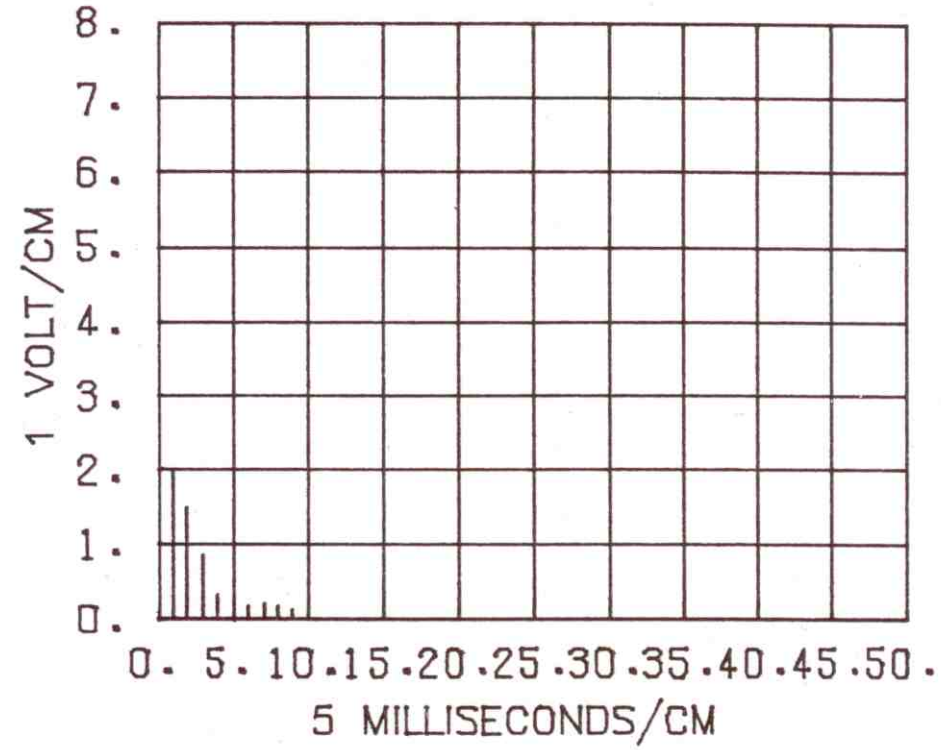

Figure C-17. Simulated Double Stage MTI Canceller Response to an Interfering Pulse (SCV-25 Mode)

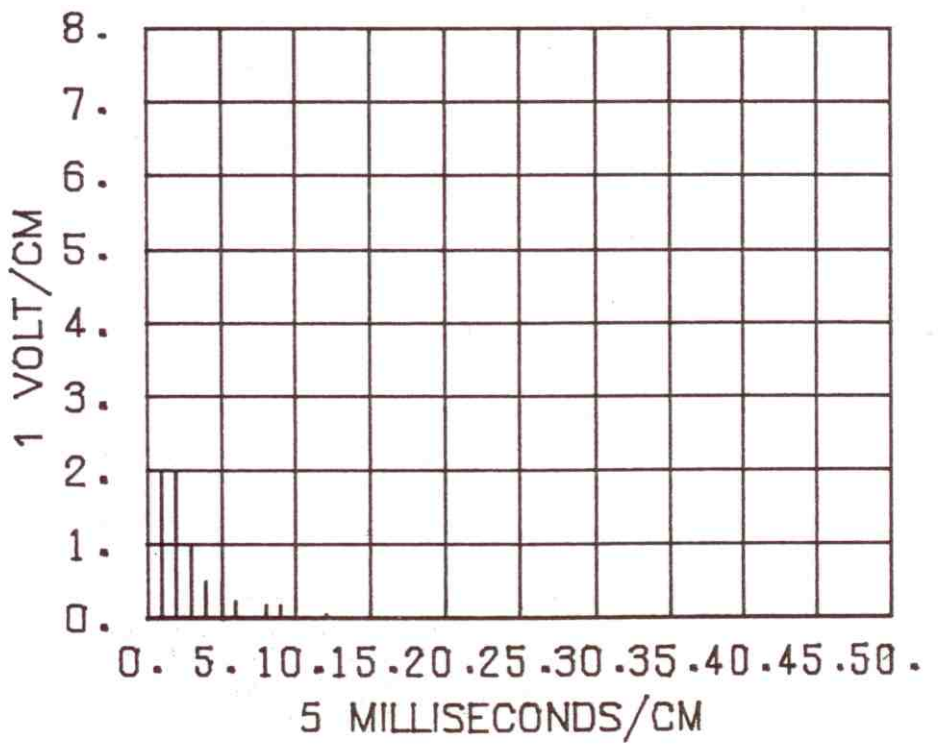

Figure C-18. Simulated Double Stage MTI Canceller Response to an Interfering Pulse (SCV-30 Mode)

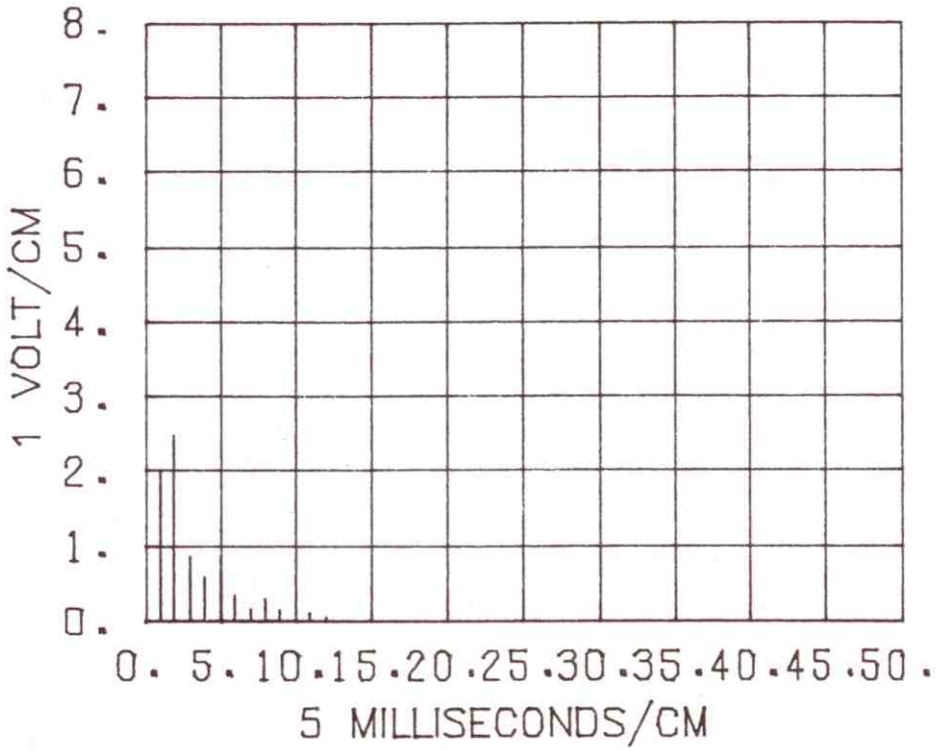

Figure C-19. Simulated Double Stage MTI Canceller Response to an Interfering Pulse (SCV-35 Mode)

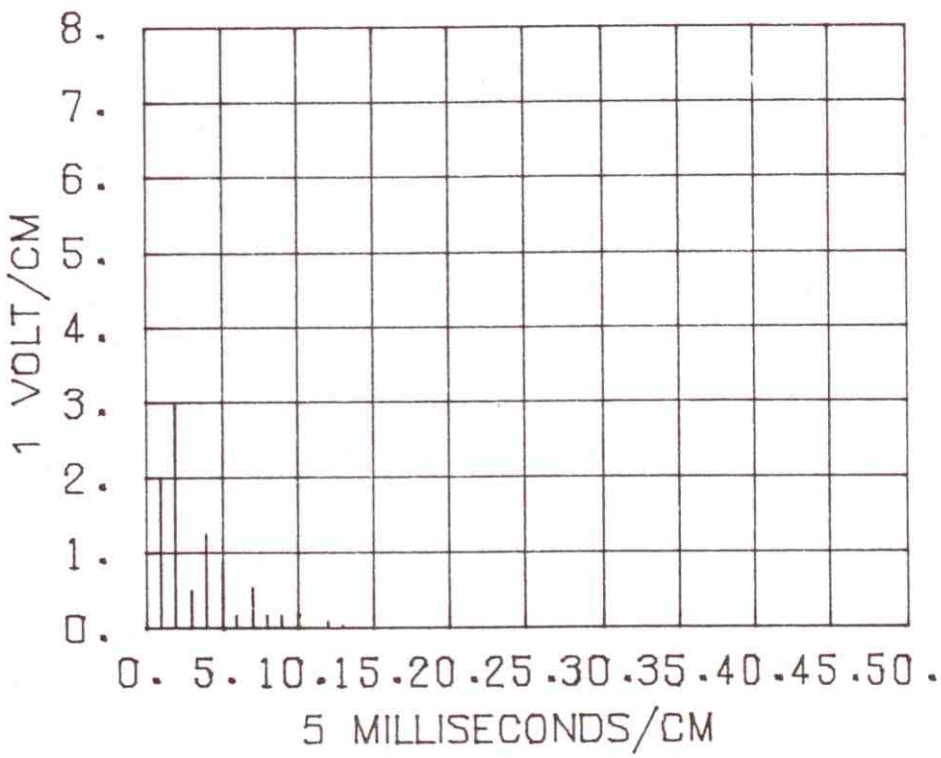

Figure C-20. Simulated Double Stage MTI Canceller Response to an Interfering Pulse (SCV-40 Mode)

power transfer properties for each of the MTI canceller modes are shown in TABLE C-1 along with the INR transfer properties of the various MTI canceller feedback modes.

RECTIFIER

The output of the MTI canceller circuits are fed to a full-wave rectifier in analog radars or an absolute value algorithm in digital radars to convert the bipolar video at the canceller output to unipolar. The rectifier output signal-to-noise ratio (SNR) is the same as at the rectifier input. The noise amplitude distribution at the full-wave rectifier output will be one-sided Gaussian since the noise amplitude at the MTI canceller output was Gaussian. The noise amplitude PDF at the rectifier output is given by:

$$p(v) = \frac{2}{\sqrt{2\pi}\sigma} e^{-v^2/2\sigma^2} \quad ; \; o \leq v \leq \infty \qquad \text{(C-40)}$$

where:

σ = rms noise level, in volts

The desired signal-plus-noise amplitude distribution PDF at the single channel MTI rectifier output for a double stage MTI canceller is shown in Figure C-21. It should be noted that the rectifier output signal-plus-noise amplitude distribution PDF shown in Figure C-21 is for the radar operating in the staggered mode and the signal averaged over all possible doppler frequencies. The PDF shown in Figure C-21 was obtained by simulation. Although the signal-plus-noise amplitude distribution PDF at the rectifier output is not of the nature of a one-sided Gaussian distribution, it can be approximated by:

$$p(v,A) = \frac{2}{\sqrt{2\pi(\sigma^2+A^2/2)}} e^{-v^2/2(\sigma^2+A^2/2)} \quad ; \; o \leq v \leq +\infty \qquad \text{(C-41)}$$

where:

σ = rms noise level, in volts

A = Desired signal amplitude, in volts

Figure C-22 shows a plot of Equation C-41 for comparison with the

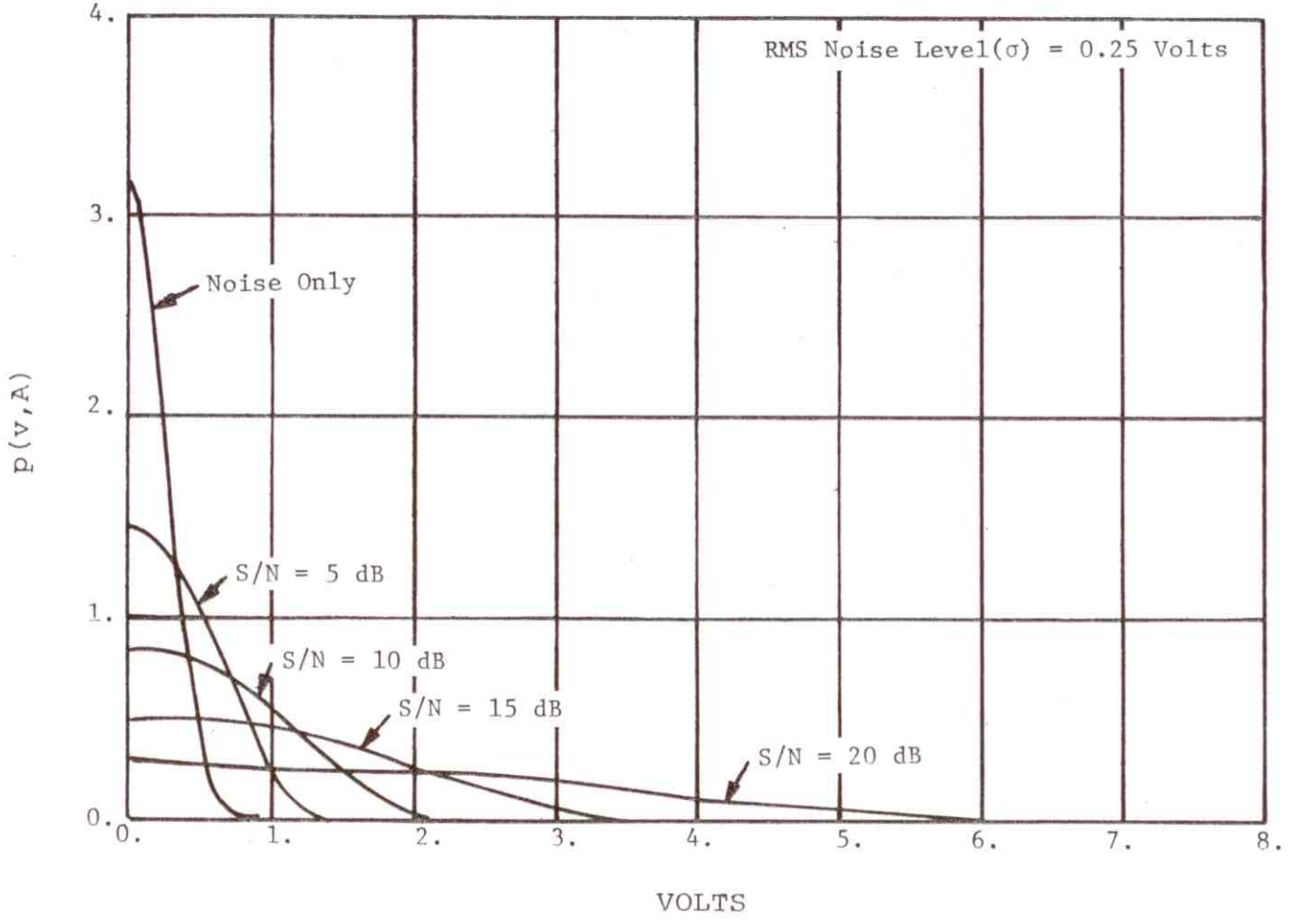

Figure C-21. Probability Density Function for Noise Only and for Signal-Plus-Noise at the MTI Canceller Output for a Single Channel Double Stage Canceller (Simulated).

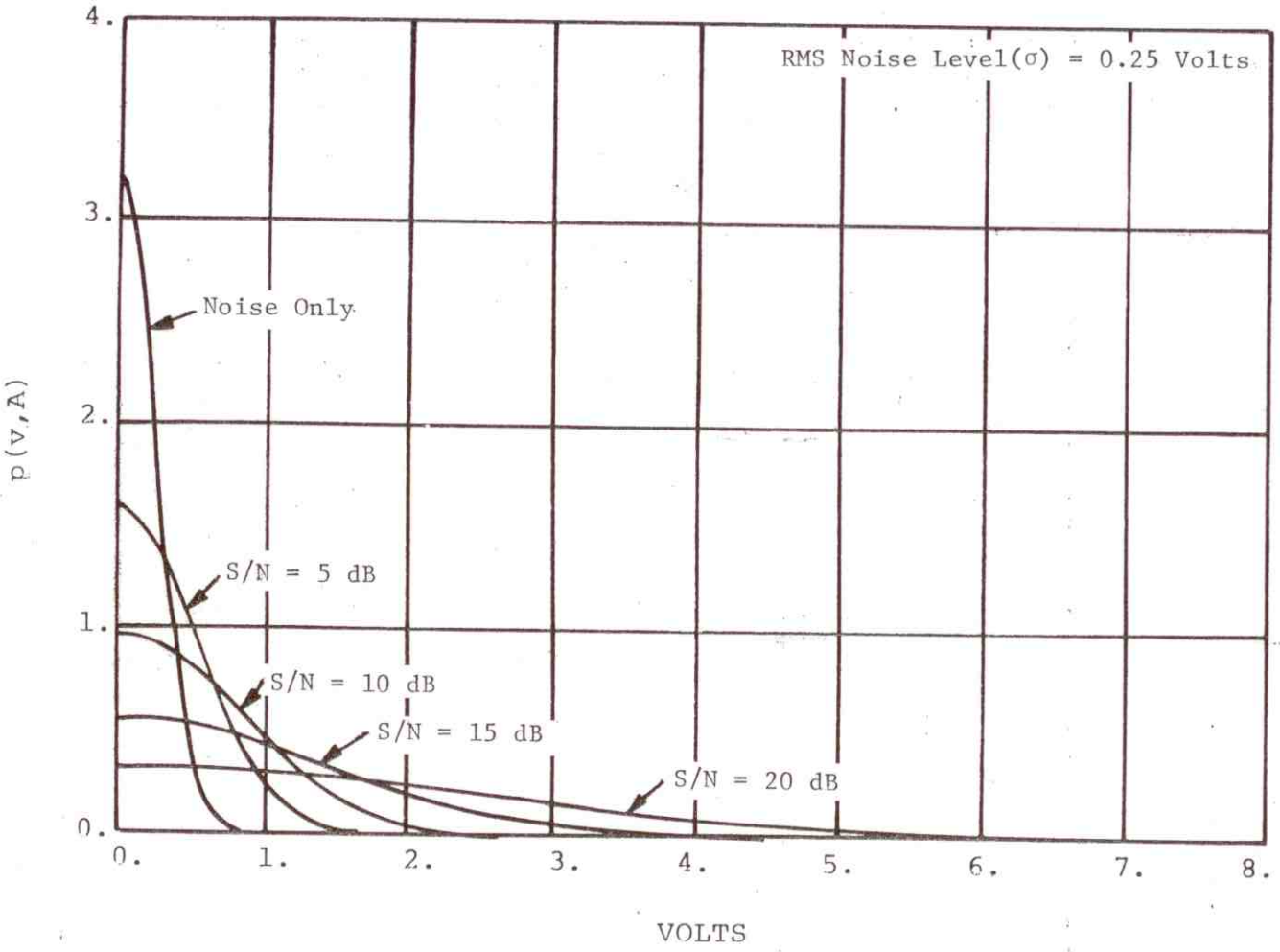

Figure C-22. Probability Density Function of One-Sided Gaussian Distribution (Equation C-41).

simulated single channel MTI rectifier output signal-plus-noise amplitude distribution PDF shown in Figure C-21.

DUAL MTI CHANNEL TRANSFER PROPERTIES

Figure C-2 shows a block diagram of a dual channel (inphase and quadrature) MTI radar. The signal transfer properties of the inphase and quadrature channels are identical to the single channel transfer properties previously discussed. The output of each channel is combined in the following manner:

$$R = \sqrt{(I)^2 + (Q)^2} \qquad \text{(C-42)}$$

Circuit implementation to achieve Equation C-42 in the combiner is complex. Often a simplified approximation to Equation C-42 is implemented by summing the larger vector amplitude with one-half the smaller vector amplitude as shown below:

$$R = |I| + |Q/2| \text{ if } |I| > |Q|$$
$$R = |Q| + |I/2| \text{ if } |I| \leq |Q| \qquad \text{(C-43)}$$

The noise amplitude distribution at the output of a dual MTI canceller is Rayleigh since the transfer properties of the combiner (Equation C-42) are similar to an envelope detector. The desired signal-plus-noise amplitude distribution PDF at the dual channel MTI combiner output for a double stage MTI canceller is shown in Figure C-23. It should be noted that the combiner output signal-plus-noise amplitude distribution PDF shown in Figure C-23 is for the radar operating in the staggered mode and the signal averaged over all possible doppler frequencies. The PDF shown in Figure C-23 was obtained by simulation. Although the signal-plus-noise amplitude distribution PDF at the combiner output is not of the nature of a Rayleigh distribution, it can be approximated by:

$$p(v,A) = \frac{v}{(\sigma^2+A^2/2} \, e^{-v^2/2(\sigma^2+A^2/2)} \quad ; \quad o \leq v \leq +\infty \qquad \text{(C-44)}$$

where:

σ = rms noise level, in volts

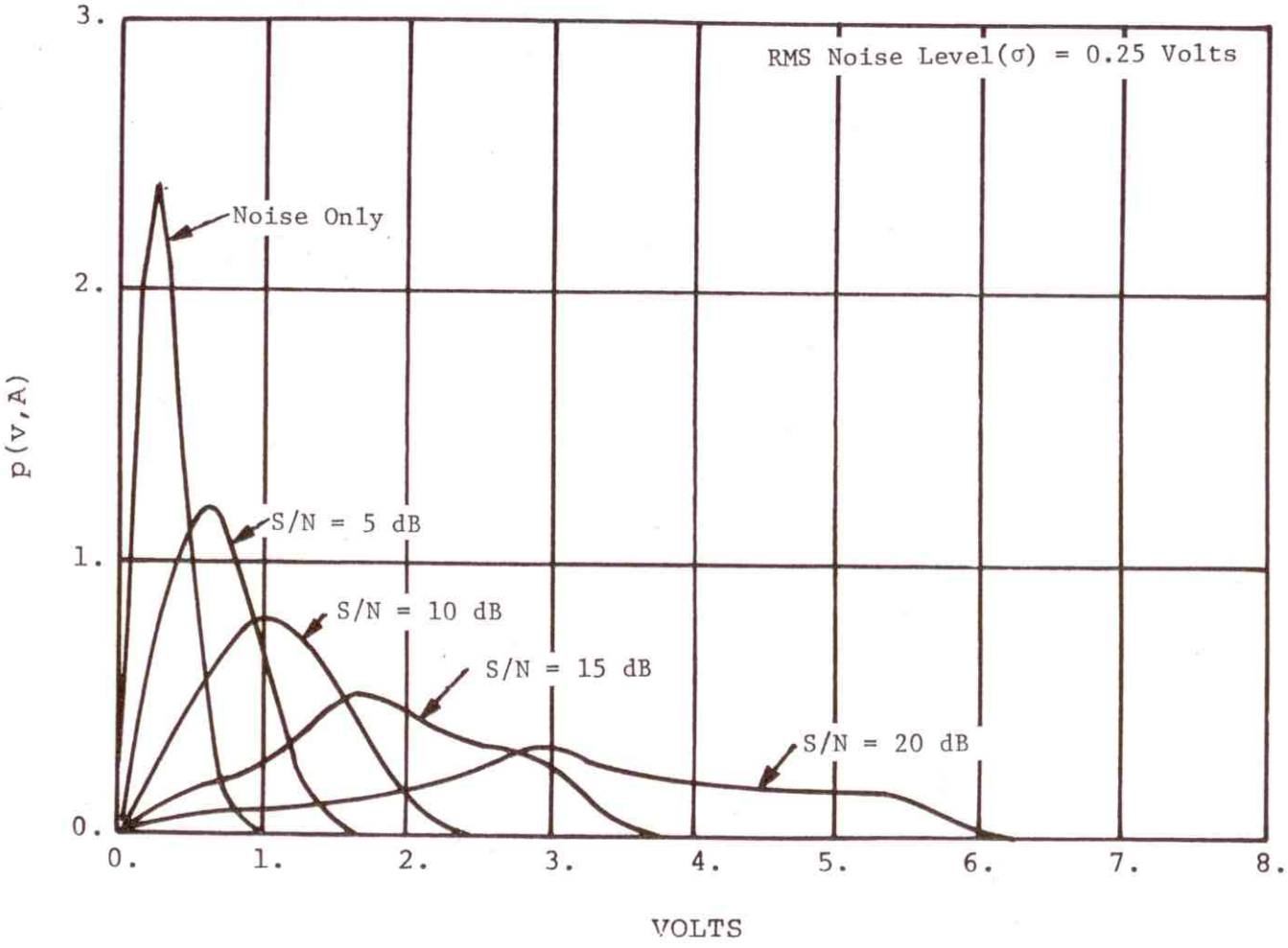

Figure C-23. Probability Density Function for Noise Only and for Signal-Plus-Noise at the MTI Canceller Output for a Dual Channel Double Stage Canceller (Simulated).

A = Desired signal amplitude, in volts

Figure C-24 shows a plot of Equation C-44 for comparison with the simulated dual channel MTI combiner output signal-plus-noise amplitude distribution PDF shown in Figure C-23.

The fact that dual MTI cancellers have the COHO reference signal of the inphase and quadrature channels phase shifted by 90 degrees, and the method in which the two channels are combined, a signal-to-noise ratio (SNR) improvement is achieved over a single MTI channel. The SNR improvement of dual MTI channels over a single MTI channel was investigated (Nathanson and Luke, 1972), and is shown in TABLE C-2. The table shows the SNR improvement for a single pulse (unintegrated pulse train) as a function of probability of false alarm (P_f) and probability of detection (P_d). For an asynchronous interfering signal, the INR enhancement of a dual MTI channel over a single MTI channel is approximately 1 to 2 dB at MDS.

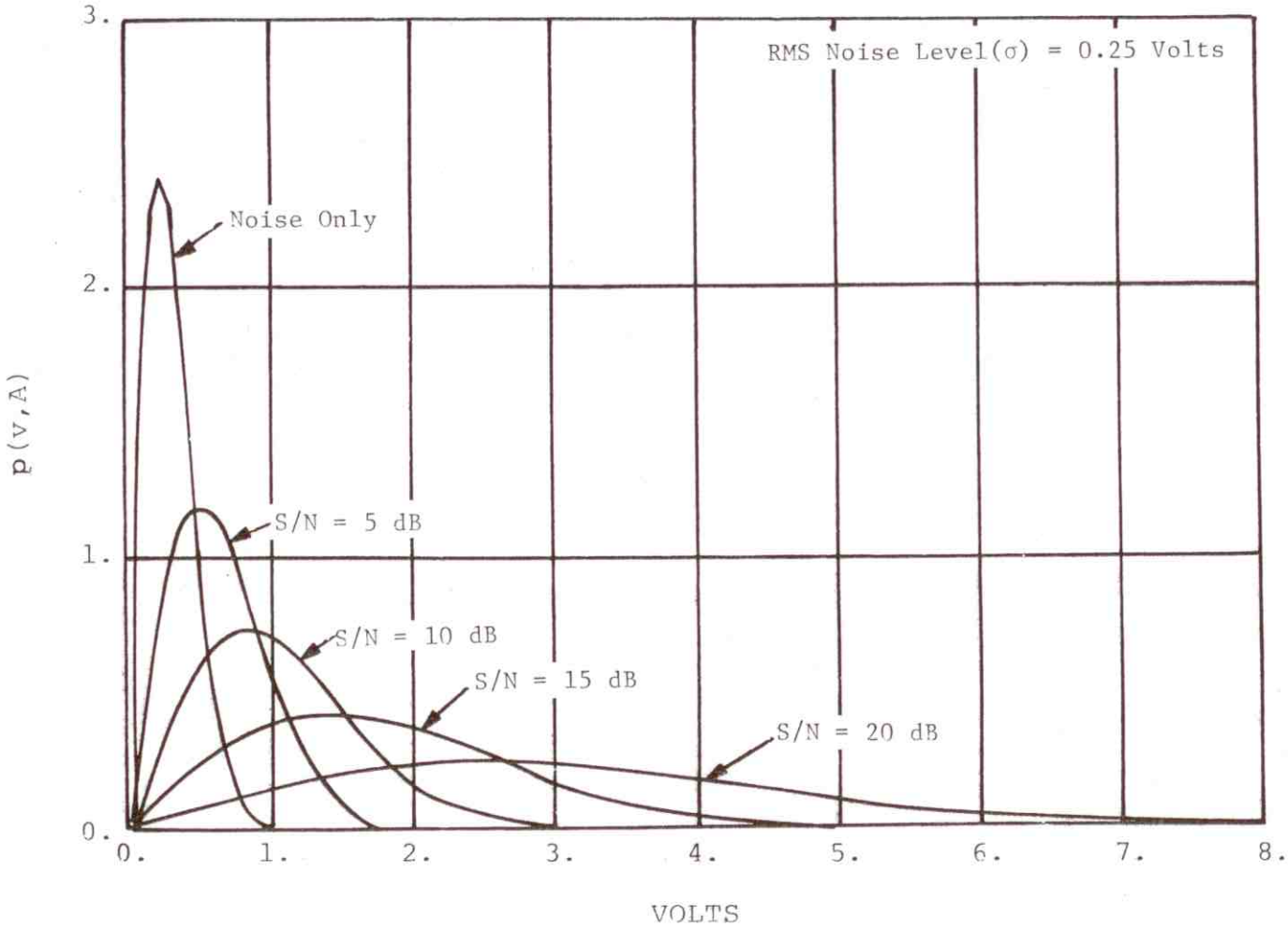

Figure C-24. Probability Density Function of Rayleigh Distribution (Equation C-44).

TABLE C-2

SIGNAL-TO-NOISE IMPROVEMENT (IN DECIBELS) RELATIVE TO DETECTION OF $I^2 + Q^2$ (FLUCTUATING SIGNAL), SINGLE PULSE

	|I| Only or |Q| Only						
P_d \ P_f	10^{-1}	10^{-2}	10^{-3}	10^{-4}	10^{-6}	10^{-8}	10^{-10}
0.5	3.29	3.81	4.05	4.19	4.35	4.45	4.51
0.8	6.45	7.17	7.48	7.66	7.86	7.97	8.04
0.9	9.12	9.92	10.26	10.45	10.66	10.78	10.85
0.95	11.95	12.79	13.14	13.34	13.56	13.68	13.76